JAERI-M
7885

INVESTIGATION ON PHYSICAL PROBLEMS IN THE IGNITION APPROACH OF D-T BURNING PLASMA BY ONE-DIMENSIONAL TOKAMAK SIMULATION CODE WITH FIXED DISTRIBUTION

September 1978

Masayoshi SUGIHARA, Masao KASAI,*
Teruhiko TAZIMA and Toru HIRAOKA

日本原子力研究所
Japan Atomic Energy Research Institute

JAERI-M 7885

Investigation on Physical Problems in the Ignition Approach of D-T Burning Plasma by One-Dimensional Tokamak Simulation Code with Fixed Distribution

Masayoshi SUGIHARA, Masao KASAI*, Teruhiko TAZIMA
and Toru HIRAOKA
Division of Large Tokamak Development, Tokai, JAERI

(Received September 1, 1978)

Physical problems to be solved in the ignition approach qf next-generation large tokamaks with NbTi toroidal field coils have been investigated preliminarily by a one-dimensional tokamak simulation code with fixed distribution.

(1) If the trapped particle instabilities are excited as predicted theoretically, the small energy confinement time will make the size of tokamak with NbTi toroidal coil considerably large to reach the ignition. If the trapped particle instabilities are suppressed to one-tenth, a moderate-sized device can achieve the ignition.

(2) Neutral beam injection using the conventional positive ions of present-day technology is insufficient to heat the plasma to the ignition. Therefore, improvement of the machine design to obtain larger injection port area, the use of an additional heating method such as RF heating together with NBI, or development of the negative ion source will be necessary.

(3) The heavy metal impurity content must be suppressed to the level of 0.01%.

Keywords: Large Tokamak, One-Dimensional Simulation, Impurity, Trapped Particle Instability, Ignition Approach, Plasma Heating

---

* On leave from Mitsubishi Atomic Power Industry Inc., Ohmiya, Saitama.

JAERI－M　7885

分布固定一次元トカマクシミュレーションコードによるＤＴ燃焼プラズマの立ち上げに関する物理的検討

日本原子力研究所東海研究所大型トカマク開発部
杉原正芳　笠井雅夫*　田島輝彦　平岡　徹

（1978年9月1日受理）

捕捉粒子不安定性によるスケーリング則を組み込んだ分布固定の一次元トカマクシミュレーションコードを用いて，JT－60の次世代の大型トカマク装置で自己点火条件の検証を目ざした時に起ると予想される物理的問題点の予備的検討を行なった。それらは次の通りである。

(1) 捕捉粒子不安定性が理論による予想通りに起ったとすると，エネルギー閉じ込め時間は短くなり，NbTiの超電導トロイダルコイルを用いた装置では，自己点火を達成する為の装置寸法は相当に大きくなると予想される。捕捉粒子不安定性が理論値の1/10程度に抑えられれば，現実的な大きさの装置で自己点火に到達させる事ができる。

(2) 現在の技術水準の正イオンを用いた中性粒子入射加熱法では，追加熱に必要なパワーを得るには不十分であると思われる。より大きな入力パワーを得るための装置設計の改良，または他の加熱法の併用，或いは負イオン源の開発等が必要と考えられる。

(3) 重金属不純物の混入量は0.01％台に抑える必要がある。

＊三菱原子力工業（株）外来研究員

Contents

目　　次

1. Introduction

One of the main purposes of the next generation tokamak to JT-60, which is now under construction in JAERI, will be to examine the ignition condition. However, under the present situation where experiments have been made only on small or medium-sized tokamak devices, it is very difficult to have perspectives for attainability of self-sustaining plasmas in the next generation large tokamak for the following reasons.

First of all, since various energy confinement scaling laws by present experiments have been derived in joule heating phase, it is quite uncertain whether or not they will be applicable to future higher temperature plasmas. A transport theory predicts that the trapped particle instabilities will be excited in future higher temperature tokamak plasmas and that they will determine transport coefficients in the tokamak. Therefore, it is of primary concern to investigate the ignition approach of the tokamak of realistic size with transport coefficients determined by trapped particle instabilities. It should be borne in mind, however, that these theoretical scaling laws are obtained by making a rough approximation of the nonlinear theory, so that it is rather ambiguous to what extent they can describe the real situation. Secondly, although the neutral beam injection heating is considered to be most reliable at present, this method for heating the plasma has an obvious drawback that the input power per unit volume decreases as the size of the device becomes large or as the plasma density increases. Thus, it is necessary to evaluate the required power to heat the plasma to ignition and to investigate whether the neutral beam injection heating can supply this required power. Thirdly, as the plasma temperature increases, energy interactions of plasma with the limiter and the first wall will strongly be enhanced. As a result, the plasma may be much more contaminated by impurities, and the energy loss due to the impurities may heavily deteriorate the energy confinement than in the present device. Therefore, it is very important to assess an allowable level of the impurity content to reach the ignition, and also to investigate the possibility of various methods for suppressing and removing impurities to this level.

In this paper, we clarify preliminarily these physical problems associated with the ignition approach in next generation large tokamak machines with NbTi superconducting toroidal magnet, using a one dimensional time dependent tokamak simulation code with fixed spatial distribution. Since the theoretically predicted trapped particle mode scaling has a

certain ambiguity, we investigate two cases; in one case theoretical trapped particle mode scaling itself is used, and in the other case one-tenthly suppressed trapped particle mode scaling is used. We also use the empirical expressions for available injection power and for energy loss due to impurities.

2. Simulation Code

2.1 Basic equations

The one-dimensional time dependent tokamak simulation code with fixed distribution calculates the time development of the space-averaged physical quantities such as density and temperature of each species, fixing their spatial profiles. Detailed descriptions of the code are presented in Ref. (13). In the present paper, we will describe the outline. We assume an axisymmetric cylindrical plasma. Basic equations for the particle balance are given as follows.

$$\frac{d\bar{n}_e}{dt} = \frac{1}{V}\left(-\Gamma_e^* + S_D + S_h + S_T\right) , \tag{2.1}$$

$$\frac{d\bar{n}_D}{dt} = \frac{1}{V}\left(-\Gamma_D^* + S_D + S_h - S_f\right) , \tag{2.2}$$

$$\frac{d\bar{n}_T}{dt} = \frac{1}{V}\left(-\Gamma_T^* + S_T - S_f\right) , \tag{2.3}$$

$$\frac{d\bar{n}_\alpha}{dt} = \frac{1}{V}\left(-\Gamma_\alpha^* + S_f\right) . \tag{2.4}$$

Equation (2.1) is for the electron density. The term Γ_e^* is electron particle flux due to diffusion. The asterisk represents that we estimate this particle flux on a certain magnetic flux surface at r*, The terms S_D, S_T and S_h on the right hand side denote the sources from deuteriums (D), tritiums (T) and injected neutrals, respectively. Equations (2.2) and (2.3) are for D and T respectively. The term S_f is the sink due to the fusion reaction. Equation (2.4) is for α-particles. In the present case, since impurity content is assumed to be very small, $n_e = n_D + n_T + 2n_\alpha$ always holds. The effects of impurities are taken into account only on the energy balance, assuming a certain impurity content depending on the plasma temperature.

Basic equations for the energy balance are

certain ambiguity, we investigate two cases; in one case theoretical trapped particle mode scaling itself is used, and in the other case one-tenthly suppressed trapped particle mode scaling is used. We also use the empirical expressions for available injection power and for energy loss due to impurities.

2. Simulation Code

2.1 Basic equations

The one-dimensional time dependent tokamak simulation code with fixed distribution calculates the time development of the space-averaged physical quantities such as density and temperature of each species, fixing their spatial profiles. Detailed descriptions of the code are presented in Ref. (13). In the present paper, we will describe the outline. We assume an axisymmetric cylindrical plasma. Basic equations for the particle balance are given as follows.

$$\frac{d\bar{n}_e}{dt} = \frac{1}{V}\left(-\Gamma_e^* + S_D + S_h + S_T\right) , \tag{2.1}$$

$$\frac{d\bar{n}_D}{dt} = \frac{1}{V}\left(-\Gamma_D^* + S_D + S_h - S_f\right) , \tag{2.2}$$

$$\frac{d\bar{n}_T}{dt} = \frac{1}{V}\left(-\Gamma_T^* + S_T - S_f\right) , \tag{2.3}$$

$$\frac{d\bar{n}_\alpha}{dt} = \frac{1}{V}\left(-\Gamma_\alpha^* + S_f\right) . \tag{2.4}$$

Equation (2.1) is for the electron density. The term Γ_e^* is electron particle flux due to diffusion. The asterisk represents that we estimate this particle flux on a certain magnetic flux surface at r*. The terms S_D, S_T and S_h on the right hand side denote the sources from deuteriums (D), tritiums (T) and injected neutrals, respectively. Equations (2.2) and (2.3) are for D and T respectively. The term S_f is the sink due to the fusion reaction. Equation (2.4) is for α-particles. In the present case, since impurity content is assumed to be very small, $n_e = n_D + n_T + 2n_\alpha$ always holds. The effects of impurities are taken into account only on the energy balance, assuming a certain impurity content depending on the plasma temperature.

Basic equations for the energy balance are

$$\frac{3}{2}\frac{d}{dt}(\bar{n}_e k \bar{T}_e) = \frac{1}{V}(- W^*_{Xe} - W^*_{ce} + W_J + W_{he} + W_{fe} - W_{ei} - W_{cy} - W_\ell) , \quad (2.5)$$

$$\frac{3}{2}\frac{d}{dt}(\bar{n}_i k \bar{T}_i) = \frac{1}{V}(- W^*_{Xi} - W^*_{ci} + W_{hi} + W_{fi} + W_{ei} - W_{cex}). \quad (2.6)$$

Equation (2.5) expresses energy balance for electron. Each term on the right hand side represents energy loss due to conduction and convection, joule heating input, input due to neutral beam injection, α-particle heating, collisional energy relaxation between ions and electrons, cyclotron radiation loss and energy losses due mainly to impurities, respectively. The last one includes bremsstrahlung radiation loss, ionization and excitation loss. These terms of energy losses and gains are obtained by integrating over the plasma volume the corresponding quantities on each mesh point which are calculated using the given density and temperature distribution. Equation (2.6) expresses energy balance for ion. Since the relaxation time between D and T ions is much shorter than the characteristic time scale of the phenomena under consideration, we assume that the equality $T_D = T_T$ holds always. The last term of the right hand side denotes the energy loss due to the charge exchange between hot plasma ions and cold neutrals. For simplicity, we assume that there are no orbit loss of energetic α-particles and injected neutrals, and that plasmas are heated by these energetic particles instantaneously.

2.2 Transport coefficients

In the present day tokamaks, with temperatures being at most 2 keV, ion energy transport can be interpreted by the neoclassical transport theory, whereas electron energy transport and particle diffusion are larger than the values predicted by this theory by a factor of several hundreds. Various confinement scaling laws have been proposed[1,2,3] to interpret experimental data. However, all the experiments so far have been made on relatively low temperature plasmas, so that it is uncertain that these scaling laws will be applicable to the future higher temperature plasma.

It is predicted theoretically, that trapped particle instabilities, which are excited by a group of particles trapped between the local magnetic mirrors, will dominate the transport coefficients in future tokamak plasmas

with high temperature.[4] In this paper, we will adopt these theoretical transport coefficients in the simulation code.

Schematical formulations for the transport coefficients used are shown in Fig. 1 with ν_{ei}, electron-ion collision frequency, as a parameter.[5] In region I, where ν_{ei}/ε (inverse aspect ratio) is larger than ω_{be} (trapped electron bounce frequency), there are few trapped particles. Thus, in this region, the ion energy transport coefficient χ_i takes the neoclassical value (plateau or Pfirsh-Schlüter), and the electron heat transport coefficient χ_e and the particle diffusion coefficient D take the neoclassical values multiplied by anomaly factors γ_χ and γ_D respectively. We determine γ_χ and γ_D, so that they interpret experimental data well. In the present case, we set $\gamma_\chi = 1000$ and $\gamma_D = 400$.[12] In regions, where $\nu_{ei}/\varepsilon < \omega_{be}$, D and χ are dominated by trapped particle instabilities. In regions II and III, the dissipative trapped electron instabilities are dominant, while in region IV are the dissipative trapped ion instabilities. Since ions do not contribute to the excitation of the dissipative trapped electron instabilities, ions energy transport coefficient is considered to be still determined by the neoclassical theory. Besides, since this instability is excited mainly by the temperature gradient, first of all it causes anomalous electron heat loss. When there is no temperature gradient, the instability is driven by the magnetic curvature drift due to the gradient of the toroidal magnetic field. In this case, the growth rate of the instability becomes smaller than that driven by the temperature gradient by a factor of ε. Thus, in regions II and III, the particle diffusion coefficient D is given as $D \sim \varepsilon\chi_e$. In region III, where ν_{ei} is smaller than that in region II, it has been proposed that the instability would be enhanced, if we take account of the curvature drift resonance, as a result of which transport coefficients would not decrease as ν_{ei} decreases.[6] In the present case, however, we will not adopt this theory. The dissipative trapped ion instability is considered to be a kind of drift wave instability of which mediums are both trapped ions and trapped electrons. The effect of Coulomb binary collisions on trapped electrons is responsible for the excitation of the instability, while that on trapped ions contributes to the damping of the wave. Thus, in this case ions as well as electrons contribute to the excitation of the instability, so that both ion and electron heat transports are dominated by this mode. Moreover, this instability is driven mainly by the density gradient, so that $\chi_e \sim \chi_i \sim D$ hold in this

region. The summary of the transport coefficients mentioned above is shown in Table 1. In the simulation code, we evaluate the collision frequency at each mesh point, in order to determine to which region the plasma belongs, and derive the transport coefficients in the region determined.

2.3 Neutral beam injection heating

The most reliable method for additional heating up to this time may be the neutral beam injection. Thus, we will adopt this method to further heat the plasma. For simplicity, we make the following assumptions.

(1) The particles to be injected are deuterons.

(2) The injection energy is assumed to be of order 150 $\sim$ 200 keV.

In the future large tokamak, the plasma minor radius a becomes large, while the attenuation length of the beam becomes short since the plasma density must become high. Therefore, higher beam energy is required so as for the plasma not to be heated near the plasma surface only.

(3) Maximum available injection power per unit volume P_{inj} is empirically given as

$$P_{inj} = 2.5/\sqrt{V} \qquad (MW/m^3) \ , \tag{2.7}$$

where V is the plasma volume.

This assumption comes from the fact that as the beam energy becomes high, the efficiency of the neutralization of the charged beam drops rapidly[7], and the fact that the ratio of the surface to the volume falls off as a^{-1}. Let us evaluate the total injection power P_{total} by Eq. (2.7) of the two devices presently under construction. In JT-60, $P_{total} \sim 20$ MW ($V = 60$ m^3), and in ISX, $P_{total} \sim 2.5$ MW ($V = 1$ m^3). These are in good agreement with their design values.

(4) The loss of the injected particles is ignored. The plasma is assumed to be heated instantaneously (ignoring the slowing down process) and uniformly over the plasma cross section.

2.4 Energy loss due to impurities

We make the following assumptions in order to calculate the energy loss due to the impurities.

(1) Impurity content increases in proportion to the mean plasma ion temperature.

We make this assumption taking account of the fact that the principal cause of the impurity generation is the sputtering of the wall by the ions outflowing from the plasma and charge exchanged hot neutral particles, as well as the fact that the sputtering yield is a sharply rising function of the energy of the bombarding particles.

(2) The expression for the energy loss per unit volume due to the impurity is given as[8)]

$$P_{loss} = 3.2 \times 10^{-36} \, f \, n_e^2 M^2 \quad (W/m^3), \tag{2.8}$$

where f and M are the fraction and atomic mass number of the impurity, respectively.

This expression includes excitation loss, ionization loss, and bremsstrahlung radiation loss. Ionization loss includes the radiative recombination loss as well as the dielectronic recombination loss. In low temperature region, ionization and excitation losses are dominant, while in high temperature region bremsstrahlung radiation loss is dominant. As a result, the radiation energy loss due to the impurities is a weakly dependent function on the local temperature as a whole. When weakly dependent function on the local temperature as a whole. When f is so small that P_{loss} becomes smaller than the bremsstrahlung radiation loss, P_{brem}, given by

$$P_{brem} = 1.42 \times 10^{-38} \, \bar{Z} \, n_e^2 \, T_e^{1/2} \quad (W/m^3), \tag{2.9}$$

where $\bar{Z}$ is the effective charge of the plasma, we use Eq. (2.9) for the radiation loss from the plasma. It should be borne in mind, however, that Eq. (2.8) rather underestimates the total radiation energy loss due to the impurities, since it takes into account only the known lines of excitation potential.[8)] Using Eq. (2.8), we find $P_{loss} \sim 0.1$ MW/m^3, when the plasma with $n_e = 1 \times 10^{20}$ m^{-3} is contaminated by molybdenum of 0.03%, or iron of 0.1%.

3. Ignition Approach

We will examine various physical problems in the ignition approach using the one-dimensional with fixed distribution time dependent simulation code described above. As for the density and temperature profile, we employ the probable profile in the present day tokamak experiments. Thus, we use Eq. (3.1) for the density, which gives a rather moderate gradient.

$$n(r) = n_o[1 - (\frac{r}{r_p})^4] + n(r_p) \quad , \tag{3.1}$$

where r_p is the radius of the plasma. Present experiments show that the temperature profile is always steeper than the density's. Thus, we use the following profile for the temperature.

$$T(r) = T_o[1 - (\frac{r}{r_p})^4]^{2.5} + T(r_p) \quad . \tag{3.2}$$

We set $r^* \sim 2a/3$, where r^* is the radius of the magnetic flux surface on which we estimate the particle and heat fluxes.

Setting the density and temperature profile and r^* in this way, we make simulations of the following two cases.

Case I: In the first case we determine the device parameter, using the widely used trapped ion mode scaling[5]. This scaling is given as

$$2n\tau = 1.78 \times 10^{37} a^4 \beta_{pe}^2 \frac{\ln\Lambda(1+\tilde{T})^2}{\tilde{T}_e^{11/2} A^{3/2}} B_t^6 \quad (s\cdot m^{-3}), \tag{3.3}$$

where $\ln\Lambda$ and β_{pe} are Coulomb logarithm and poloidal beta by electron, respectively. B_t is toroidal magnetic field at plasma center. In Eq. (3.3), we have taken into account the energy loss due to the convection as well as the conduction, whereas in Ref. (5) they are not taken into account correctly. In the future tokamak reactor, the use of superconducting toroidal magnet is inevitable. At present, the development of Nb_3Sn superconducting magnet seems to take more time than that of NbTi. So we decide to use NbTi superconducting magnet as toroidal coils. Toroidal magnetic field at plasma center B_t is given as

$$B_t = B_{max} (1 - \frac{1 + \Delta/a}{A}) \quad , \tag{3.4}$$

where B_{max} and Δ are the maximum available magnetic field at the inner surface of the coil and the distance between the plasma surface and the inner surface of the toroidal coil. We set B_{max} = 8 tesla for NbTi superconducting magnet. Setting Δ = 1.2 m, A = 4.5 and $\beta_p \sim 2.8$, the device parameters to reach the ignition at 8 keV of $\bar{T}_i$ are given as follows.

a (plasma minor radius) = 1.8 m

R (plasma major radius) = 8.2 m

B_t (magnetic field at plasma center) = 5 tesla

I_p (plasma current) = 4 MA

P_{total} (maximum injection power) $\sim$ 72 MW

The direct application of Eq. (3.3) requires such a large device when NbTi superconducting magnet is used.

Figure 2 shows the result of simulation of the ignition approach of this device. It is assumed that the plasma is free from impurities. The mode of operation is that the plasma current rises up to 4 MA in one second after the start up, and after 2 seconds the neutral beam injection heating is started until after 16 seconds. During the injection, cold neutrals are also puffed into the plasma in order to increase the plasma density, keeping each D and T component always equal. In about half second after the start of the neutral beam injection, the plasma temperature rises up to about 5 keV, and the plasma parameter enters the region of trapped ion mode (region IV) since the density is still low. In this region, since the (region IV) since the density is still low. In this region, since the energy confinement time τ_E is proportional to the plasma density, and since the energy input per one particle from the injection is inversely proportional to the plasma density, the temperature rising becomes independent of the density. Thus, the plasma temperature saturates at about 5.5 keV. This situation continues until after 8 seconds. After 8 seconds, the plasma parameter enters the trapped electron mode region (III) due to the increase of the collision frequency ν_{ei}. Since, in this region, the confinement time τ_E is inversely proportional to the density, the confinement deteriorate as the density increases. In this way, the temperature falls rapidly and the ignition cannot be reached. As can be understood from this result, in order to reach the ignition, the temperature must somehow be risen more. The temperature saturation is determined by the balance between the injection power and the energy confinement of the trapped ion mode scaling.

Therefore, the temperature dependence of the confinement time of the trapped ion mode scaling, that is to say $\tau_E \propto T^{-7/2}$, is quite severe for temperature rising. In fact, in order to raise the temperature by 50%, an order of magnitude larger injection power is required, or the confinement should be improved by an order of magnitude. In the present case, however, we can expect the α-particle heating to be effective to reach the ignition, if it is possible to raise the temperature up to 6 ∿ 7 keV. Thus, as a reference study, we make a simulation assuming that larger injection power can be available.

Figure 3 shows the result with larger injection power. Total injection power, P_{total} = 126 MW, heats the plasma from 2 seconds to 16 seconds. No impurity contents are assumed. As a result, the plasma temperature rises to about 6.5 keV, and we find that at 12 ∿ 13 seconds the ignition is attained. However, it should be noted that the poloidal beta value becomes 7 ∿ 8 when the ignition is reached. In other words, the confinement time determined by the trapped ion mode scaling is so short that such a high beta value is required to reach the ignition. Although this value exceeds the critical value for the equilibrium of circular plasma, the poloidal beta value might be reduced within a critical value by employing non-circular plasma. Furthermore, with the present day engineering level it seems to be difficult to inject such a high power as more than 120 MW in the present model device. There might be an obvious geometrical limitation of increasing the ratio of the total injection port area to the plasma surface area. The beam current density may also be restricted by the space charge limit. Therefore, such a high power injection using the conventional positive ion beam may be difficult. The improvement of the machine design to obtain larger ratio of the injection port area to the plasma surface area, or the development of a negative ion source, which has fairly high neutralizing efficiency even for high energy beams, or the use of other further heating methods such as RF heating together with the neutral beam injection will be required.

Although we have determined the device parameters using the trapped ion mode scaling Eq. (3.3), we find that it is difficult to reach the ignition in this device. The discrepancy comes from the fact that Eq. (3.3) might rather overestimate $n\tau$ value, since it has been obtained by making approximations that $\frac{1}{n}\frac{\partial n}{\partial r} \sim \frac{1}{T}\frac{\partial T}{\partial r} \sim \frac{1}{a}$ and so on. For example, if the plasma density and temperature are parabolic,

$$n\tau = 3.16\times10^{33}\left(\frac{a}{r}\right)^{12.5}\frac{1}{\left[1-\left(\frac{r}{a}\right)^2\right]^{8.25}}\frac{a^4\beta_{pe}^2\ln\Lambda(1+\tilde{T})^2 B_t^{\,6}}{\bar{T}^{11/2}A^{3/2}q^4} \quad (s\cdot m^{-3}) \qquad (3.5)$$

In fact, this value of $n\tau$ is one-second or third as large as Eq. (3.3) when $r \sim 2a/3$. Thus, if we aim the ignition when the trapped ion instabilities are really excited as theoretically predicted, the plasma minor radius may be required 2 meters or more. This plasma size seems to be unrealistically large.

Case II: As the second example, we investigate the ignition approach in a smaller device.[9] The device parameters are

$$a = 1.4\ \text{m},\quad R = 6.3\ \text{m},\quad A = 4.5,$$
$$I_p = 3\ \text{MA},\quad B_t = 4.7\ \text{tesla},\quad P_{total} = 42\ \text{MW}.$$

If the trapped particle instabilities are really excited as theoretically predicted, this smaller device than that in Case I may be unable to reach the ignition. It should be borne in mind, however, that the scaling law by trapped particle instabilities has been obtained by making a rough approximation in solving the nonlinear equation, so that its coefficient may include an order of magnitude ambiguity. Furthermore, Ohkawa recently pointed out that if the electromagnetic effect due to the finite beta is taken into account, the growth rate of the dissipative trapped ion instability is reduced by a factor of $1/A^2$.[10] In addition, Clarke obtained the result that, in fusing plasma at equilibrium state, the plasmas adjust themselves their density profiles so as to become broad and temperature profiles sharp, as a result of which the growth rate of the dissipative trapped ion instability is about one-tenthly reduced.[11] Therefore, we will investigate whether these smaller device parameters can give an ignition or not by using the simulation code with transport coefficients by trapped particle instabilities being one tenthly suppressed. Figure 4 shows the ignition approach without impurity contamination. We start the neutral beam injection after 2 seconds from the start up, and continue it until 12 seconds. After $9 \sim 10$ seconds from the start up, the self-sustaining state is achieved. Again, however, the poloidal beta value

exceeds the critical value when the ignition is reached (β_p = 5 ∿ 6). In this case, β_p value will be rather easily reduced within a critical value by shaping the plasma cross section to ellipse, or employing Nb_3Sn superconducting toroidal magnet.

Next, we investigate the effect of impurities in this device. Figure 5 shows the ignition approach, in which the plasma is assumed to be contaminated by molybdenum impurities of 0.01% when $\bar{T}_i$ = 1 keV and 0.1% when $\bar{T}_i$ = 10 keV. Considering the fact that, even in the present day tokamaks, of which ion temperature are of order 1 keV, the plasmas are contaminated by heavy metal impurities of about 0.1%, some methods for the suppression of impurity contamination will be required in order to achieve 0.1% contamination at $\bar{T}_i$ = 10 keV. After 2 seconds, at which the beam injection is started, the plasma is in the trapped ion region up to 7 seconds. Thereafter, as the plasma particle density n is increased, the energy loss due to the impurities becomes large in proportion to n^2. Thus the temperature falls off rapidly and the ignition cannot be achieved. From this result we can conclude that the content of heavy metal impurities such as molybdenum should be suppressed to the order of 0.01% when $\bar{T}_i$ = 10 keV.

Let us consider the suppression of the impurity content by some means of the magnetic divertor, honeycomb liner and so on. Even if we assume that the cause of the impurity generation is only the sputtering of the wall by hot neutral particles with about 1 keV, which are generated by the charge exchange with the recycling neutrals, the efficiency of the suppression of impurities by means of the impurity removal by the magnetic divertor and the suppression of the effective sputtering yield by the honeycomb liner is required to be 98% or more.[12] Furthermore, if we consider other causes of impurity generation such as sputtering by plasma ions, self-sputtering by molybdenum ions, evaporation and so on, the problem of the impurity suppression will be more severe. Thus, some methods for controlling the plasma boundary by using the divertor, cold gas blanket, other potential materials such as low Z materials or light metals for the limiter and the first wall with being maintained at low temperature, and so on will be necessary.

So far we have investigated the ignition approach by using one-tenthly suppressed trapped particle mode scaling in this smaller device. Even if the trapped particle modes occur as theoretically predicted, we can expect the ignition in this smaller device by employing Nb_3Sn superconducting toroidal coils which make us expect better confinement by an order of

magnitude. In addition, the condition for impurity suppression could be fairly relaxed.

4. Conclusions

We investigated various physical problems during the ignition approach of D-T burning plasma by using the one-dimensional time dependent tokamak simulation code with fixed spatial distribution, in which the scaling laws by trapped particle instabilities were incorporated. The problems to be overcome in order to achieve the ignition can be summarized as follows.

(1) If the trapped particle instabilities are really excited as theoretically predicted, the energy confinement time would be very short and larger plasma minor radius of 2 meters or more will be required to reach the ignition when NbTi superconducting toroidal magnet is used. Particularly, the strong temperature dependence of the transport coefficients by the trapped ion instability severely prevents temperature rising.

(2) It may be rather difficult to supply a sufficient power to heat the plasma by a neutral beam injection using the conventional positive ions of the present day engineering level. An improvement of the machine design to obtain larger injection port area, or the use of other additional heating methods such as RF heating together with NBI, or the development of the negative ion source will be necessary.

(3) In the case, where heavy metal, such as molybdenum, is used for the limiter or the first wall, the content of heavy metal impurities should be suppressed to a level of 0.01% for a higher temperature plasma of next generation. Some methods will be required to remove the impurities, to suppress the impurity influx and to lower the effective sputtering yield in order to achieve this requirement. Potential use of low Z materials or light metals for the limiter and the first wall should be examined.

These are not independent problems, but are related to each other. For instance, if a sufficient heating power is available, at least during the start up phase to the ignition, the allowable level of the impurity content is relaxed to a certain extent. The similar effect can be expected if the confinement time determined by the trapped particle instabilities becomes longer than that predicted theoretically.

magnitude. In addition, the condition for impurity suppression could be fairly relaxed.

4. Conclusions

We investigated various physical problems during the ignition approach of D-T burning plasma by using the one-dimensional time dependent tokamak simulation code with fixed spatial distribution, in which the scaling laws by trapped particle instabilities were incorporated. The problems to be overcome in order to achieve the ignition can be summarized as follows.

(1) If the trapped particle instabilities are really excited as theoretically predicted, the energy confinement time would be very short and larger plasma minor radius of 2 meters or more will be required to reach the ignition when NbTi superconducting toroidal magnet is used. Particularly, the strong temperature dependence of the transport coefficients by the trapped ion instability severely prevents temperature rising.

(2) It may be rather difficult to supply a sufficient power to heat the plasma by a neutral beam injection using the conventional positive ions of the present day engineering level. An improvement of the machine design to obtain larger injection port area, or the use of other additional heating methods such as RF heating together with NBI, or the development of the negative ion source will be necessary.

(3) In the case, where heavy metal, such as molybdenum, is used for the limiter or the first wall, the content of heavy metal impurities should be suppressed to a level of 0.01% for a higher temperature plasma of next generation. Some methods will be required to remove the impurities, to suppress the impurity influx and to lower the effective sputtering yield in order to achieve this requirement. Potential use of low Z materials or light metals for the limiter and the first wall should be examined.

These are not independent problems, but are related to each other. For instance, if a sufficient heating power is available, at least during the start up phase to the ignition, the allowable level of the impurity content is relaxed to a certain extent. The similar effect can be expected if the confinement time determined by the trapped particle instabilities becomes longer than that predicted theoretically.

We can expect that Nb_3Sn superconducitng toroidal magnet provides a better confinement by an order of magnitude than NbTi toroidal magnet.

It should be borne in mind that these conclusions are derived on the basis of the fixed distribution simulation code. If we take account of the variation of profiles of the various plasma parameters, there remains a possibility that these conclusions are modified to a certain extent.

At any rate, these physical problems will be investigated experimentally in various medium-sized devices, such as PLT and so on, in the coming several years. It should be of primary importance to have perspectives for the attainability to the ignition by the tokamak type device of realistic size, with continuous reference to these experimental results.

Acknowledgments

The authors express their thanks to Drs. M. Yoshikawa, Y. Iso and S. Mori for their continuing encouragements throughout this work.

References

1) C. Daughney: Nuclear Fusion 15 (1975) 967.
2) E. Apgar, et al.: Proc. 6th Int. Conf. Plasma Physics and Controlled Nuclear Fusion Research, Berchtesgaden, (1976) 1, IAEA, Vienna (1977) 247.
3) J. Hugill and J. Sheffield: Nuclear Fusion 18 (1977) 15.
4) B.B. Kadomtsev and O.P. Pogutse: Nuclear Fusion 11 (1971) 67.
5) S.O. Dean et al.: WASH-1295 (1974).
6) D.F. Düchs, D.E. Post and P.H. Rutherford: Nuclear Fusion 17 (1977) 565.
7) K.H. Berkner, T.J. Morgan, R.V. Pyle and J.W. Stearns: Physical Review A 8 (1973) 2870.
8) T. Tazima, Y. Nakamura and K. Inoue: Nuclear Fusion 17 (1977) 3.
9) T. Hiraoka, M. Sugihara, M. Kasai and S. Mori: Proc. 2nd IAEA Conference and Workshop on Fusion Reactor Design, Madison.
10) T. Ohkawa: GA-A14273 (1977).
11) J. Clarke: ORNL/TM-5860 (1977).
12) T. Tazima: JAERI-M 7717 (1978).
13) T. Tazima et al.: to be published in JAERI-M (1978).

We can expect that Nb_3Sn superconducitng toroidal magnet provides a better confinement by an order of magnitude than NbTi toroidal magnet.

It should be borne in mind that these conclusions are derived on the basis of the fixed distribution simulation code. If we take account of the variation of profiles of the various plasma parameters, there remains a possibility that these conclusions are modified to a certain extent.

At any rate, these physical problems will be investigated experimentally in various medium-sized devices, such as PLT and so on, in the coming several years. It should be of primary importance to have perspectives for the attainability to the ignition by the tokamak type device of realistic size, with continuous reference to these experimental results.

Acknowledgments

The authors express their thanks to Drs. M. Yoshikawa, Y. Iso and S. Mori for their continuing encouragements throughout this work.

References

1) C. Daughney: Nuclear Fusion 15 (1975) 967.
2) E. Apgar, et al.: Proc. 6th Int. Conf. Plasma Physics and Controlled Nuclear Fusion Research, Berchtesgaden, (1976) 1, IAEA, Vienna (1977) 247.
3) J. Hugill and J. Sheffield: Nuclear Fusion 18 (1977) 15.
4) B.B. Kadomtsev and O.P. Pogutse: Nuclear Fusion 11 (1971) 67.
5) S.O. Dean et al.: WASH-1295 (1974).
6) D.F. Düchs, D.E. Post and P.H. Rutherford: Nuclear Fusion 17 (1977) 565.
7) K.H. Berkner, T.J. Morgan, R.V. Pyle and J.W. Stearns: Physical Review A 8 (1973) 2870.
8) T. Tazima, Y. Nakamura and K. Inoue: Nuclear Fusion 17 (1977) 3.
9) T. Hiraoka, M. Sugihara, M. Kasai and S. Mori: Proc. 2nd IAEA Conference and Workshop on Fusion Reactor Design, Madison.
10) T. Ohkawa: GA-A14273 (1977).
11) J. Clarke: ORNL/TM-5860 (1977).
12) T. Tazima: JAERI-M 7717 (1978).
13) T. Tazima et al.: to be published in JAERI-M (1978).

We can expect that Nb_3Sn superconducitng toroidal magnet provides a better confinement by an order of magnitude than NbTi toroidal magnet.

It should be borne in mind that these conclusions are derived on the basis of the fixed distribution simulation code. If we take account of the variation of profiles of the various plasma parameters, there remains a possibility that these conclusions are modified to a certain extent.

At any rate, these physical problems will be investigated experimentally in various medium-sized devices, such as PLT and so on, in the coming several years. It should be of primary importance to have perspectives for the attainability to the ignition by the tokamak type device of realistic size, with continuous reference to these experimental results.

Acknowledgments

The authors express their thanks to Drs. M. Yoshikawa, Y. Iso and S. Mori for their continuing encouragements throughout this work.

References

1) C. Daughney: Nuclear Fusion 15 (1975) 967.
2) E. Apgar, et al.: Proc. 6th Int. Conf. Plasma Physics and Controlled Nuclear Fusion Research, Berchtesgaden, (1976) 1, IAEA, Vienna (1977) 247.
3) J. Hugill and J. Sheffield: Nuclear Fusion 18 (1977) 15.
4) B.B. Kadomtsev and O.P. Pogutse: Nuclear Fusion 11 (1971) 67.
5) S.O. Dean et al.: WASH-1295 (1974).
6) D.F. Düchs, D.E. Post and P.H. Rutherford: Nuclear Fusion 17 (1977) 565.
7) K.H. Berkner, T.J. Morgan, R.V. Pyle and J.W. Stearns: Physical Review A 8 (1973) 2870.
8) T. Tazima, Y. Nakamura and K. Inoue: Nuclear Fusion 17 (1977) 3.
9) T. Hiraoka, M. Sugihara, M. Kasai and S. Mori: Proc. 2nd IAEA Conference and Workshop on Fusion Reactor Design, Madison.
10) T. Ohkawa: GA-A14273 (1977).
11) J. Clarke: ORNL/TM-5860 (1977).
12) T. Tazima: JAERI-M 7717 (1978).
13) T. Tazima et al.: to be published in JAERI-M (1978).

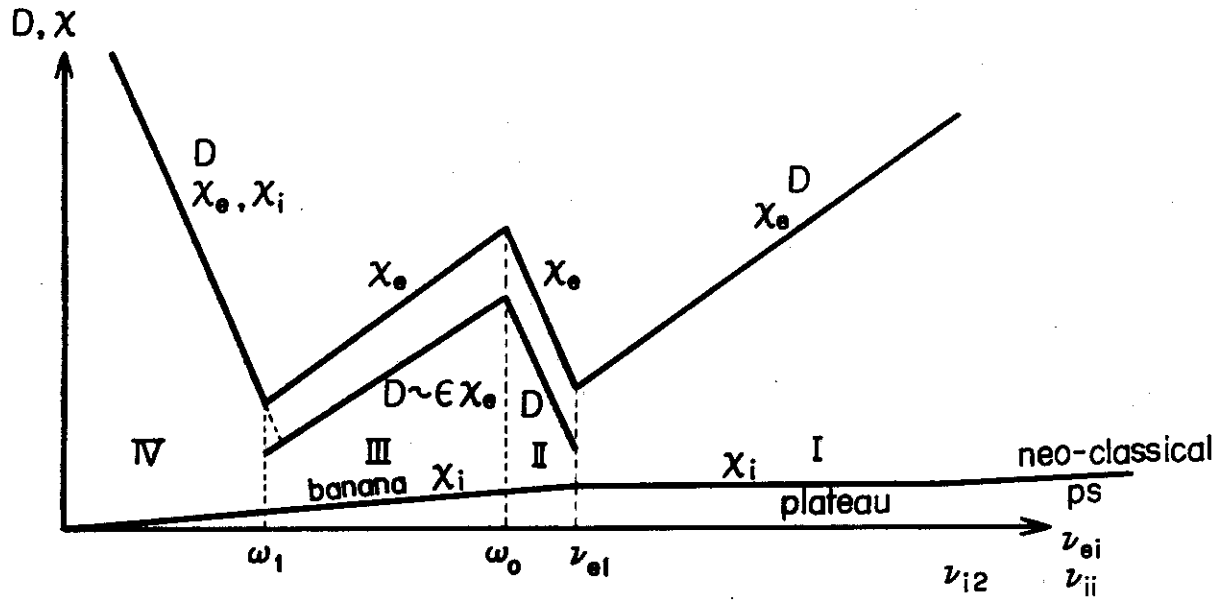

Fig. 1 Schematical formula of the scaling laws used in the simulation code.

Table 1 Summary of the scaling laws used in each region.

Region	χ_e	χ_i	D
Ⅰ	Anomaly x Classical	Neo-classical	Anomaly x Classical
Ⅱ	Trapped Electron ①	Neo-classical	Trapped Electron ①
Ⅲ	Trapped Electron ②	Neo-classical	Trapped Electron ②
Ⅳ	Trapped Ion	Trapped Ion	Trapped Ion

Transport Coefficient in Figure 1 are given as follows

Electron thermal conductivity χ_e:

$$\chi_{eI} = \gamma_\chi (1 + 1.6q^2)\rho_e^2 \nu_{ei} \quad ,$$

$$\chi_{eII} = 3\varepsilon^{3/2} r^2 \frac{\omega^*_{min} \omega^{*T}_{min}}{\nu_{ei}} \quad ,$$

$$\chi_{eIII} = 0.06\varepsilon^{1/2} \left(\frac{d \ln T_e}{d \ln n_e}\right) \frac{m_i}{m_e} \frac{B_t}{\theta B_\theta} \rho_e^2 \nu_{ei} \quad ,$$

$$\chi_{eIV} = \frac{\varepsilon^{5/2} r^2 (\omega^*_{min})^2}{\nu_{ei}(1 + T_e/T_i)^2} \quad .$$

Ion thermal conductivity χ_i:

$$\chi_{iI} = \begin{cases} (1 + 1.6q^2)\rho_i^2 \nu_{ii} & (\nu_{ii} \geq \nu_{i2}) \\ \dfrac{0.68}{1 + 0.36\nu_i^*} \varepsilon^{-3/2} q^2 \rho_i^2 \nu_{ii} & (\nu_{ii} < \nu_{i2}) \end{cases} ,$$

$$\chi_{iII} = \chi_{iI} \quad ,$$

$$\chi_{iIII} = \chi_{iI} \quad ,$$

$$\chi_{iIV} = \chi_{eIV} \quad .$$

Diffusion coefficient D:

$$D_I = \gamma_D (1 + q^2)\rho_e^2 \nu_{ei} \quad ;$$

$$D_{II} = 3\varepsilon^{5/2} r^2 \frac{\omega^*_{min} \omega^{*T}_{min}}{\nu_{ei}} \equiv \varepsilon \chi_{eIII} \quad ,$$

$$D_{III} = 0.06\varepsilon^{3/2} \left(\frac{d \ln T_e}{d \ln n_e}\right) \frac{m_i}{m_e} \frac{B_t}{\theta B_\theta} \rho_e^2 \nu_{ei} \equiv \varepsilon \chi_{eIII} \quad ,$$

$$D_{IV} = \chi_{eIV} = \chi_{iIV} \quad .$$

List of symbols in these expressions

$q = aB_t/RB_\theta$: safety factor

$\varepsilon = r/R$: inverse aspect ratio

B_t : toroidal magnetic field

B_θ : poloidal magnetic field

ν_{ei}, ν_{ii} : Coulomb collision frequency for electrons and ions.

m_j (j=i,e) : mass

v_{thj} (j=i,e) : thermal velocity

Ω_j (j=i,e) : cyclotron frequency

$\Omega_{\theta j}$ (j=i,e) : Cyclotron frequency for poloidal magnetic field

$\rho_j = v_{thj}/\Omega_j$ (j=i,e) : Larmor radius

$\rho_{\theta j} = v_{thj}/\Omega_{\theta j}$ (j=i,e) : poloidal larmor radius

$r_n = (\frac{1}{n}\frac{dn}{dr})^{-1}$: density gradient length

$L_s = (\frac{r}{q^2R}\frac{\partial q}{\partial r})^{-1}$: shear length

$\theta = r_n/L_s$: shear parameter

$\omega^*_{min} = \frac{v_{thi}}{r}\frac{\rho_i}{r_n}$: minimum diamagnetic drift frequency

$\omega^{*T}_{min} = \frac{c}{eBr}\frac{\partial T}{\partial r}$: minimum temperature drift frequency

$\ell_d = 0.06\varepsilon^{1/2}(\frac{d\ln T_e}{d\ln n_e})\frac{m_i}{m_e}\frac{B_\theta}{\theta B_t}$

$\omega_0 = \omega^*_{min}(\frac{r}{\rho_{\theta e}})(\frac{3\varepsilon^{3/2}}{\ell_d}\frac{d\ln T_e}{d\ln n_e})^{1/2}$

$\omega_1 = \omega^*_{min}(\frac{r}{\rho_{\theta e}})\frac{T_i/T_e}{1+T_i/T_e}(\varepsilon^{5/2}/\ell_d)^{1/2}$

$\nu^*_i = \nu_{ii}/\nu_{i1}$

$\nu_{j1} = \varepsilon^{3/2} v_{thj}/qR$ (j=i,e)

$\nu_{j2} = v_{thj}/qR$ (j=i,e)

γ_D, γ_χ : anomaly factor

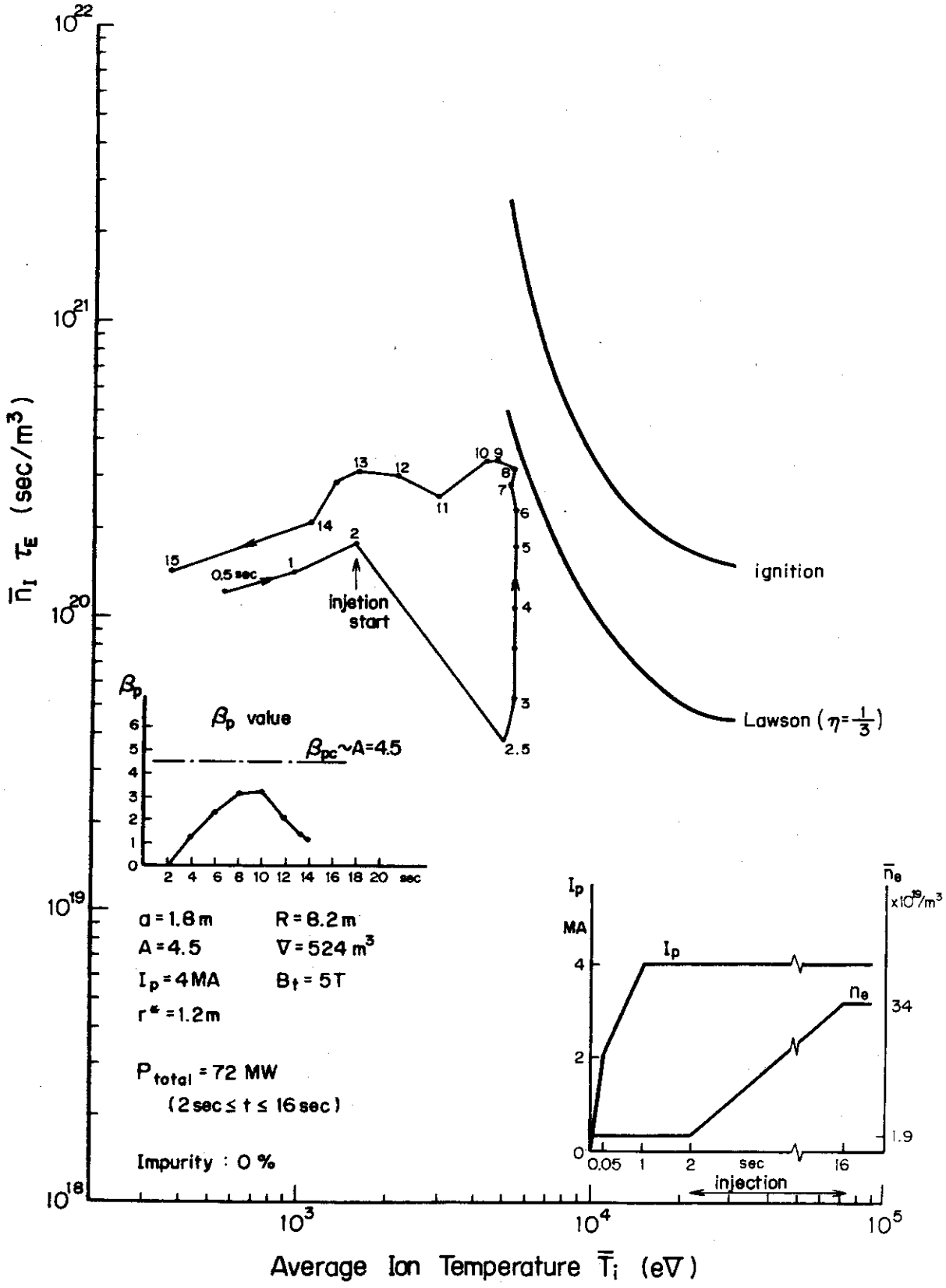

Fig. 2 Ignition approach of case I device with 72 MW injection power. No impurity contamination is assumed.

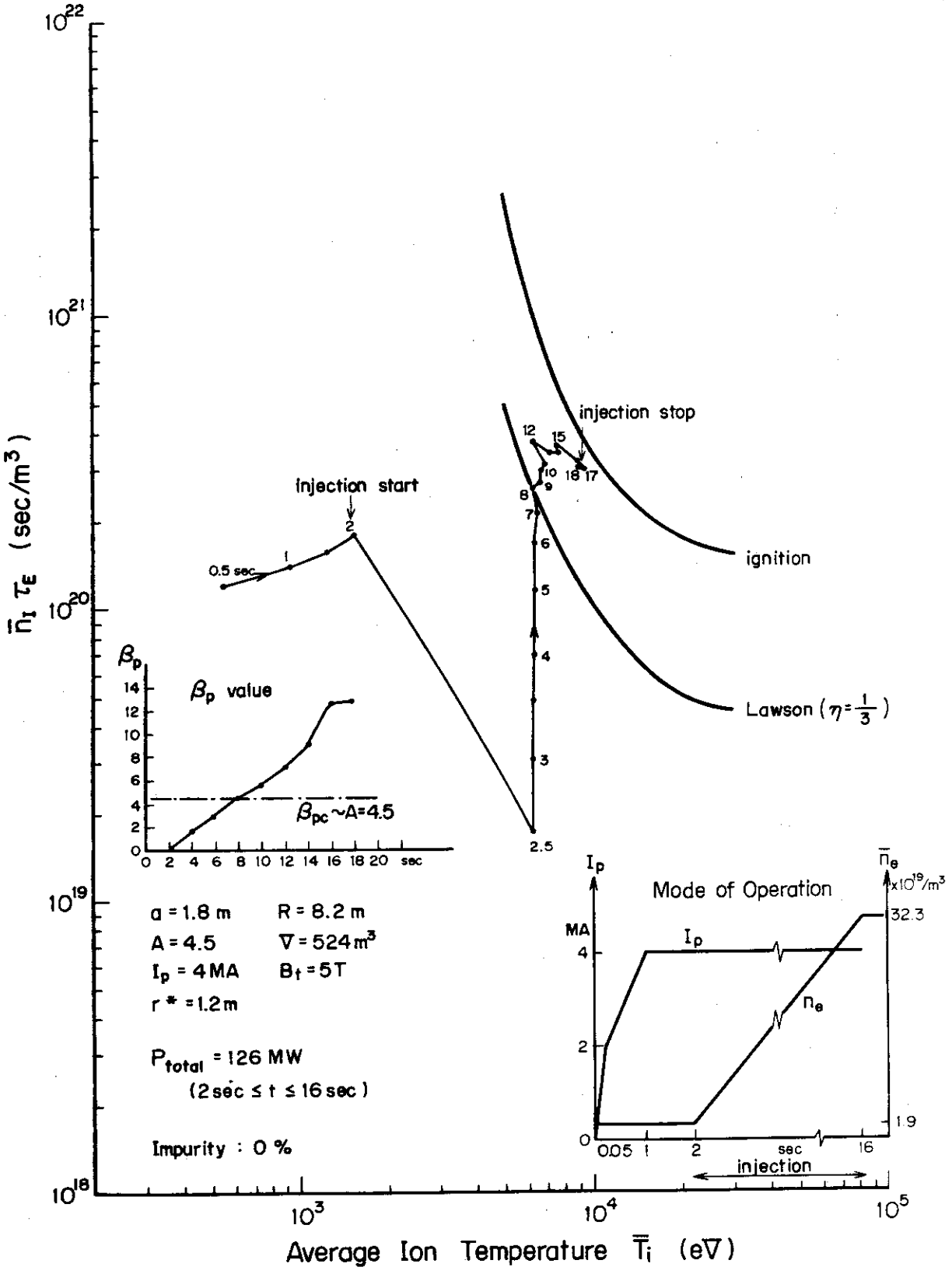

Fig. 3 Ignition approach of case I device with 120 MW injection power. No impurity contamination is assumed.

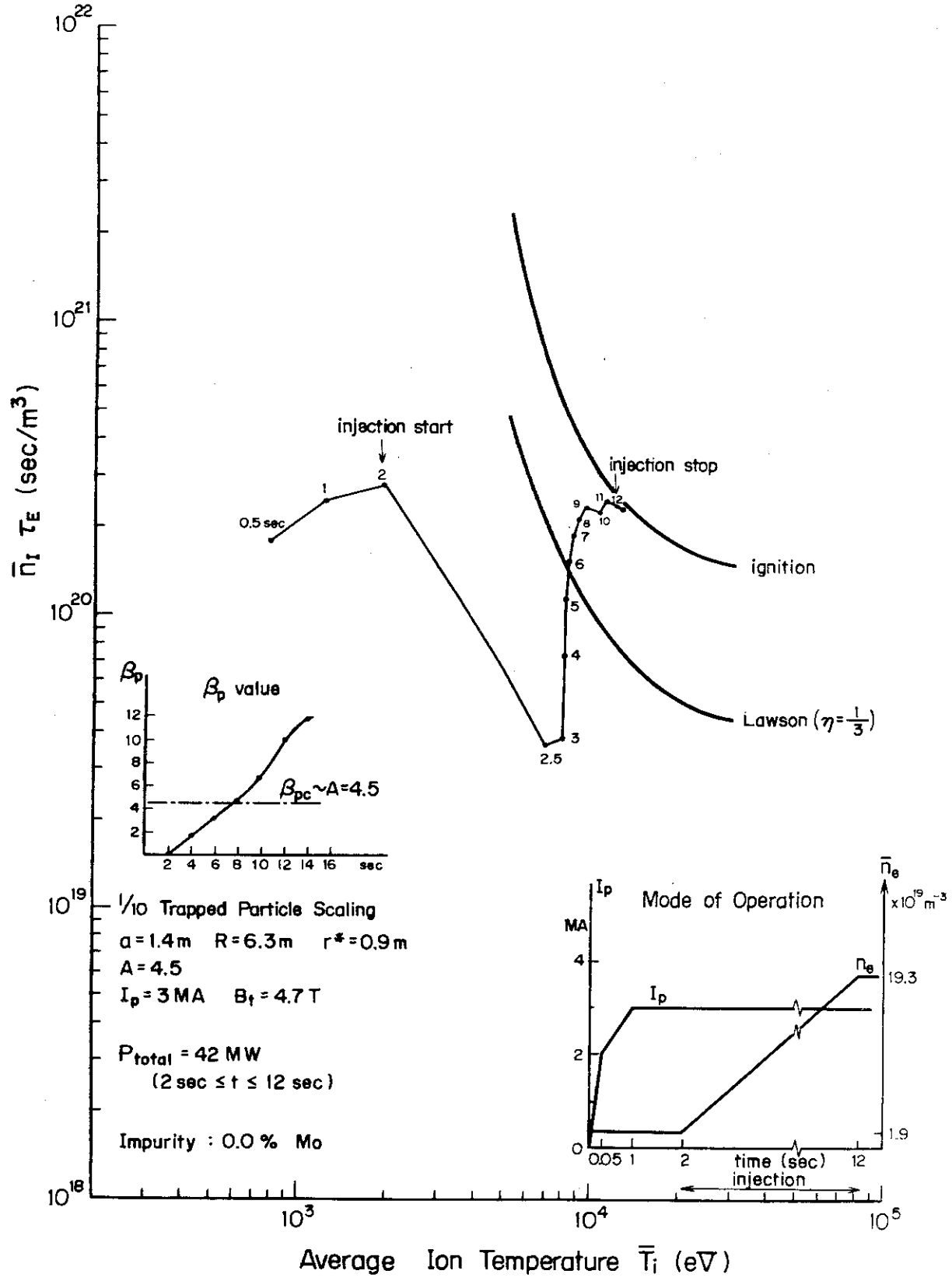

Fig. 4 Ignition approach of case II device with 42 MW injection power. Trapped particle mode scalings are suppressed to one-tenth. Plasmas are assumed to be impurity free.

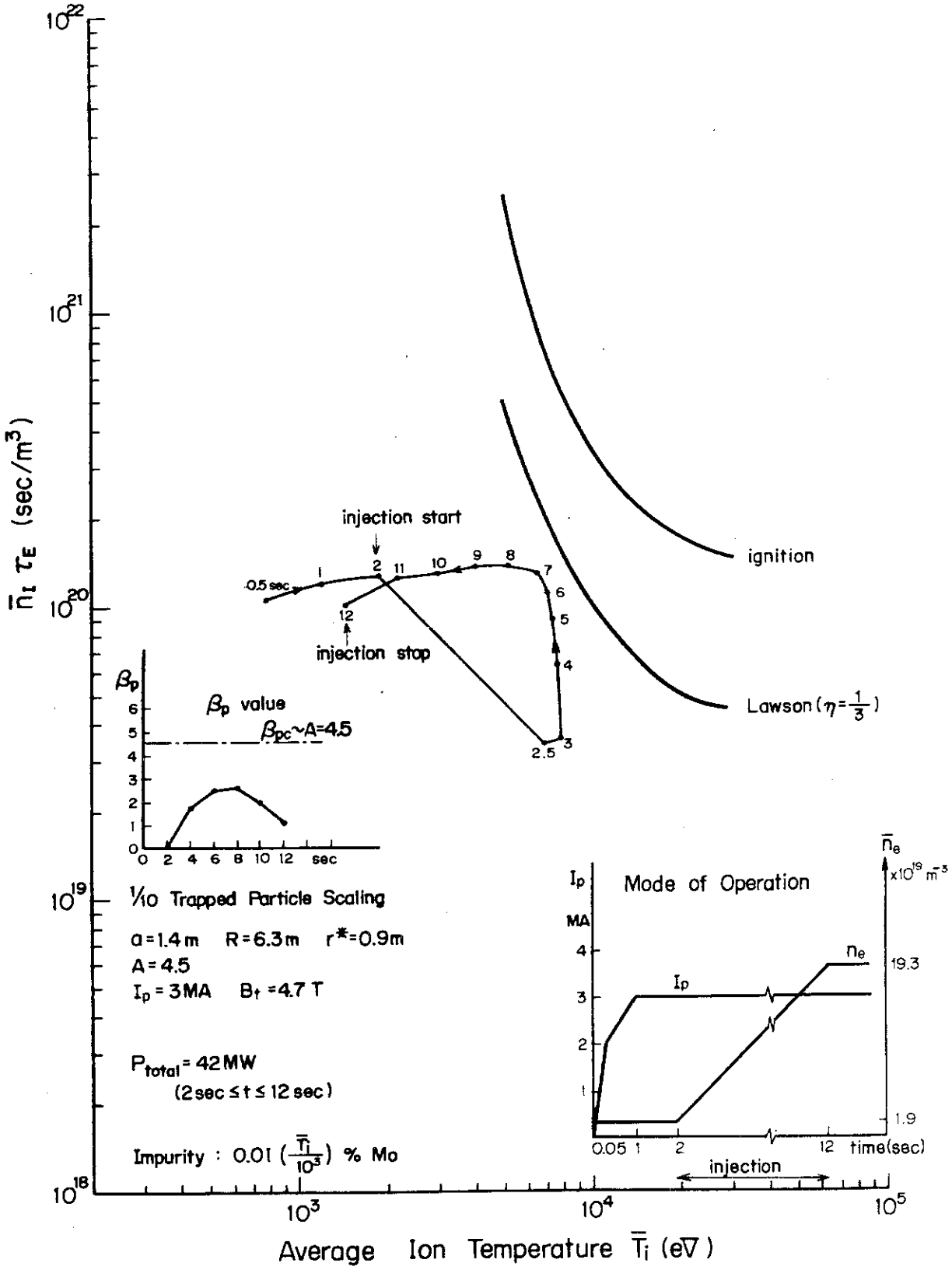

Fig. 5 Ignition approach of case II device with 42 MW injection power. Trapped particle mode scalings are suppressed to one-tenth. Plasmas are assued to be contaminated by molybdenum impurities of 0.01% at $\bar{T}_i$ = 1 keV and 0.1% at $\bar{T}_i$ = 10 keV.